# Ion-Specific and Reversible Wetting of Imidazolium-Based Minigels

**ARTICLE** *in* THE JOURNAL OF PHYSICAL CHEMISTRY B · OCTOBER 2008

Impact Factor: 3.3 · DOI: 10.1021/jp802761y · Source: PubMed



**8 AUTHORS**, INCLUDING:

Ivan Jose Suarez Suarez
@NA
**8** PUBLICATIONS **197** CITATIONS
SEE PROFILE

Bj Retama Retama
Complutense University of Madrid
**53** PUBLICATIONS **818** CITATIONS
SEE PROFILE

Enrique López-Cabarcos
Complutense University of Madrid
**156** PUBLICATIONS **2,509** CITATIONS
SEE PROFILE

Antonio Fernández-Barbero
Universidad de Almería
**97** PUBLICATIONS **1,761** CITATIONS
SEE PROFILE

# Ion-Specific and Reversible Wetting of Imidazolium-Based Minigels

**Iván J. Suárez,[†] Jorge Rubio-Retama,[‡] Benjamín Sierra-Martín,[†] F. Javier de las Nieves,[†] David Mecerreyes,[§] Enrique López-Cabarcos,[||] Manuel Márquez,[⊥] and Antonio Fernández-Barbero*,[†]**

*Group of Complex Fluids Physics, Department of Applied Physics, University of Almería, Almería 04120, Spain, Leibniz Institut für Polymerforschung Dresden e.V Hohe Strasse 6, Dresden 01069, Germany, CIDETEC, Paseo Miramon 196, 20009, San Sebastian, Spain, Department of Pharmaceutical Chemical-Physics, University Complutense of Madrid, 28040 Madrid, Spain, and NIST Center for Theoretical and Computational Nanosciences, Gaithersburg, Maryland 20899, Harrington Department of Bioengineering, Arizona State University, Tempe, Arizona 85287, and Center for Integrated Nanotechnologies, Los Alamos National Laboratory K771, Los Alamos, New Mexico 87545*

*Received: March 31, 2008; Revised Manuscript Received: May 30, 2008*

Cross-linked imidazolium-based [poly(ViEtIm$^+$Br$^-$)] microparticles were synthesized, and their wetting properties were studied by optical microscopy, after addition of aqueous solutions of sodium halides. Particle wetting showed ion specificity due to counterion binding, described by Desnoyer's model. The interaction between anions and the microparticles allowed exchanging halogenides between them in a reversible way. A salt-independent characteristic wetting time was found as well as a decreasing power law with salt concentration, for the network diffusion coefficient. It modified the polymer network elasticity as ion concentration increased, making the network softer.

## Introduction

Polymerization of imidazolium-like ionic liquids reported by Salamone et al.,[1] and more recently Onho et al.,[2,3] started a new kind of high performance materials with excellent conductivity for $Li^+$ and protons. These polyelectrolytes, usually denoted as polymer ionic liquids (PILs), become excellent candidates for the development of high charge density lithium batteries[4,5] and fuel cell devices.[6] One of the main limiting matters of nano- or microdevices is the miniaturization of the energy sources to be incorporated, making this a task of paramount importance.

Marcilla et al.[10] has proposed a new two-step route toward the synthesis of polymeric ionic liquid particles, which is adapted in the present Article for the synthesis of cross-linked imidazolium-based [poly(ViEtIm$^+$Br$^-$)] microparticles (range of micrometers). Particle swelling is studied after addition of sodium halides, showing ion specificity. The control of particle swelling is thus possible by a proper selection of the electrolyte. Swelling reversibility is shown by direct optical inspection after ion exchange cycles, becoming a reusable system precursor of industrial applications.

Particle wetting is monitored by optical microscopy. Data are analyzed using the Flory−Huggins theory with an extra ionic term accounting for the mesh charge and ion redistribution. The kinetics of swelling is tracked with a high speed camera. Tanaka's kinetic model for polymer gels is used to describe the wetting process and to extract information about the diffusion of the polymer network.[7,8]

From both the final equilibrium state and the swelling process, we find that the presence of ions in the solvent modifies the polymer solubility as well as its elasticity. This feature should be taken into account for imidazolium-based batteries or ion sensors design.[5,6,9,10]

Several specific aspects are reported and discussed in this Article concerning particle swelling: (i) the final equilibrium size after addition of electrolyte solutions, which is a consequence of the competition among mixing, elastic, and electrical contributions; (ii) the wetting kinetics, mainly related to the diffusion of the polymer network; and (iii) the ion-specific and reversible wetting.

## Experimental Section

**Imidazolium-Based Minigels.** ***Synthesis of 3-Ethyl-1-vinyl-1H-imidazol-3-ium Bromide.*** The monomer was prepared by reacting 25 mL of freshly distilled 1-vinylimidazole with 50 mL of ethyl bromide under nitrogen atmosphere at reflux conditions for 8 h. The resulting white product was subsequently filtered and washed several times with ethyl acetate. With the aim of purifying the monomer, 20 g of the previously synthesized monomer was dissolved in 5 mL of dichloromethane. This solution was added dropwise into 200 mL of cold acetone provoking the precipitation of white acicular crystals of pure 3-ethyl-1-vinyl-1*H*-imidazol-3-ium bromide. These crystals were filtered and washed with ethyl acetate and dried in vacuum.

***Synthesis of Poly(3-ethyl-1-vinyl-1H-imidazol-3-ium bromide) Minigels.*** Cross-linked poly(3-ethyl-1-vinyl-1*H*-imidazol-3-ium bromide), [poly(ViEtIm$^+$Br$^-$)], minigels are prepared with a water-in-oil (W/O) concentrated emulsion pathway.[11] *N*,*N*′-Methylene-bisacrylamide (BA) was employed as cross-linking molecule. The disperse water aqueous phase consists of 5 mL of 3.5 M of 1-vinyl-3-ethylimidazolium bromide, BA 5% mol (taking as reference the mol quantity of ViEtIm$^+$Br$^-$ monomer),

* Corresponding author. Phone: +34-950015909/950015910. Fax: +34-950015477. E-mail: afernand@ual.es.
[†] University of Almería.
[‡] Leibniz Institut für Polymerforschung.
[§] CIDETEC.
[||] University Complutense of Madrid.
[⊥] NIST Center for Theoretical and Computational Nanosciences, Arizona State University, and Los Alamos National Laboratory.

10.1021/jp802761y CCC: $40.75 
Published on Web 08/07/2008

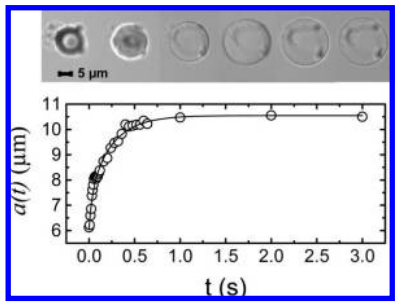


**Figure 1.** Particle radius as a function of time in the wetting process with deionized water. Pictures correspond to (from left to right): 0.0, 0.04, 0.2, 0.4, 0.6, and 2.0 s, respectively.

and the initiator ammonium persulfate (25 mg), dissolved in a phosphate buffer (pH 6) solution. The continuous oil phase consists of 250 $\mu$L of Span 80 and 750 $\mu$L of dodecane. The W/O emulsion is prepared by dropwise addition of the dispersed phase into the continuous phase. A concentrated W/O gel-like emulsion is obtained after the polymerization, which is started by addition of *N*,*N*,*N*′,*N*′-tetramethylethylenediamine (TEMED) (63 $\mu$L). The emulsion was homogenized under magnetic stirring and purged with nitrogen gas to remove any residual oxygen. After 1 h of reaction at room temperature, the minigel particles were precipitated with acetone and next isolated by filtration and washed with distilled water. After solvent separation, the miniparticles were freeze-dried to remove residual solvent and water and stored at 4 °C. The particles were redispersed in water and dialyzed before use.

***Tracking Particle Wetting.*** Particle response to different ion concentrations is directly tracked using a high-speed digital camera (RDT/16) connected to an optical microscope (Leica DMIRB). Digital video is recorded to 125 fps using standard white lighting. Picture acquisition was calibrated with an 80 lines/mm diffraction grating (PHYWE 09827.00) and a 40×/0.55 objective. To account for possible optical anisotropy, the calibration was performed in both horizontal and vertical directions. The final calibration is (0.15 ± 0.01) $\mu$m/pixel.

A drop of minigel suspension is placed on top of a glass slide and dried at room temperature. One particle is selected to perform all experiments. Particle swelling starts after addition of electrolyte solution of NaF or NaCl or NaBr or NaI (Aldrich, 99%) with concentrations in the range 0.0−1.0 M. Before a new swelling process, ions from the previous run are removed by washing with deionized water, and finally the particle is allowed to dry to set similar initial conditions.

The particle perimeter is monitored during the swelling process, and the enclosed area is calculated to determine the particle size. Figure 1 shows a typical wetting process, plotting the particle radius as a function of time. The final equilibrium size $a_f = \lim_{t\to\infty} a(t)$ is typically reached at about 1 s.

## Theory

**Gels at Equilibrium.** Polymer gels reach thermodynamic equilibrium when the solvent chemical potential is equal inside and outside the gel. Consequently, no net transfer of solvent takes place, and the difference in osmotic pressure between gel and the external aqueous phase is zero. Three features contribute to the total osmotic pressure: polymer solubility (mixing term, $\pi_m$), network elasticity (elastic term, $\pi_e$), and mesh charge (ionic term, $\pi_i$). The elastic and ionic contributions compete against each other; the first tries to shrink the gel while the second tries to swell it. The mixing contribution, however, presents an ambivalent behavior; this is determined by the value of the Flory parameter, $\chi$, describing the interaction between polymer and solvent molecules. For high polymer solubility, $\pi_m$ tries to swell the gel, while in the case of bad solvent, the mixing term is unfavorable and $\pi_m$ contributes to gel deswelling. The Flory−Huggins and Donnan theories describe and quantify the different contributions.[12–16]

The mixing osmotic pressure, $\pi_m = -(N_a kT/\upsilon_s)[\Phi + \ln(1-\Phi) + \chi\Phi^2]$, depends on the polymer volume fraction, $\Phi$, and temperature, $T$, with $N_a$ and $k$ being the Avogadro number and Boltzmann constant, respectively. $\upsilon_s$ stands for the molar volume of the solvent. Once $V_o$ and $\phi_o$ are chosen as the volume and polymer volume fraction for a reference state (usually, the collapsed state), the volume fraction, $\Phi$, is experimentally accessible for isotropic spherical gels through measurements of the gel diameter, $D$: $\Phi_r \equiv \Phi/\Phi_0 = (D_0/D)^3$, with $D_o = (6V_o/\pi)^{1/3}$ being the size of the reference state. The mixing term contributes to swelling or deswelling, depending on $\chi$. For high polymer solubility ($\chi < 0.5$), the mixing osmotic pressure increases monotonously with $\Phi$, always favoring gel swelling. At low polymer solubility ($\chi > 0.5$), the effect of the mixing contribution depends on the polymer density; the gel tries to swell for high enough polymer concentration and to deswell for even higher $\Phi$ values.

The network elasticity always contributes to gel deswelling. It is set only by the network cross-linking $N_C$ (network number of chains) and modulated through the reduced polymer volume fraction, $\Phi_r$, as $\pi_e = (N_c kT/V_0)[^1/_2\Phi_r - \Phi_r^{1/3}]$.

For ionic gels, an additional contribution describing the presence of charge is considered; it manifests through direct Coulombic repulsions among polymer chains and by the effect of the ion distribution inside and outside the gel.[14] Within the weak screening limit ($\kappa R < 1$, with $R$ the size of the polymer chain and $\kappa$ the inverse of the Debye length), the effect of counterions dominates: the network charge sets a constant electrostatic potential (Donnan potential, $U$), driving ions redistribution inside and outside the gel. An osmotic pressure is established inside the gel as a result of the unequal ion distribution. Within the weak screening limit and for high enough ion concentration, the osmotic pressure increases with the network charge, $Q$, and decreases with the ion concentration, $n$, following a power law, $\pi_i = (N_a kT/4)\Phi_r^2 Q^2 V_0^{-2} n^{-1}$, valid for $Q/V < n$. The different contributions to the total osmotic pressure do not work independently. Their relation is given by the equation of state: $\pi_{total} = \pi_m + \pi_e + \pi_i = 0$. Changes in particle size modify the different contributions to the total osmotic pressure, so that thermodynamic equilibrium is attained.

**Gels toward Equilibrium: Swelling Kinetics.** Tanaka et al. derived a model describing the swelling kinetics of a polymer gel network.[7] The displacement of a point located on the network from its final equilibrium location is represented by $u$. With this definition, $u = 0$ at time $t \to \infty$. The time dependence of $u$ determines the swelling kinetics. The equation of motion is given by Newton's second law for a continuum medium, assuming the network does not accelerate:[17] $f\,\partial\vec{u}/\partial t = \nabla\cdot\bar{\bar{\sigma}}$, where $f$ is the solvent-network friction coefficient and $\bar{\bar{\sigma}}$ is the stress tensor, $\sigma_{ik} = K\nabla\cdot u\,\delta_{ik} + 2\mu(u_{ik} - \nabla\cdot u\delta_{ik}/3)$, with $K$ and $\mu$ the bulk and shear modulus of the polymer network, respectively, and $u_{ik} \equiv {}^1/_2((\partial u_k/\partial x_i) + (\partial u_i/\partial x_k))$. This description simply establishes that forces associated with internal stresses (produced by volume changes and shear deformations) are balanced by the friction exerted by the liquid on the network. For a spherically symmetric swelling process, it becomes:[7]

$$\frac{\partial u}{\partial t} = D \cdot \frac{\partial}{\partial r}\left\{\frac{1}{r^2} \cdot \left[\frac{\partial}{\partial r}(r^2 u)\right]\right\}$$

where the magnitude of the displacement vector obeys a Fick-like diffusion equation, with $D = (K + 4\mu/3)/f$ as the gel diffusion coefficient. This equation can be solved using Fourier expansion to yield:[7]

$$a(t) = a_f - \left(\frac{6}{\pi^2}\right)\Delta a_o \cdot \sum_{n=1}^{\infty} \frac{\exp\left(-n^2 \frac{t}{\tau}\right)}{n^2}$$

$$\tau = \frac{a_f^2}{\pi^2 \cdot D} \quad (1)$$

with $\tau$ being the characteristic swelling time, $a_f$ the final equilibrium gel radius at equilibrium, and $\Delta a_o$ the total radius increase for the whole swelling process ($a_f - \Delta a_o$ corresponds to the initial radius of the gel).

## Results and Discussion

**Equilibrium after Wetting.** The final particle size after wetting is plotted in Figure 2 as a function of the NaBr concentration. The particle size decreases with increasing ion concentration as a consequence of the Donnan contribution, causing charge screening around the polymer chains.

The ionic contribution diminishes with salt concentration, being balanced by the other two osmotic contributions (mixing and elastic) to fulfill the equilibrium condition $\pi_{total} = \pi_m + \pi_e + \pi_i = 0$. The total number of chains within the gel is $N_c = 2.2 \times 10^{11}$, according to the particle synthesis. The particle charge density $Q/V$ is also calculated to be $5.04 \times 10^7$ C m$^{-3}$, assuming 100% of ionization at the working pH =5.88. The Flory solvency parameter, $\chi$, is therefore calculated as a fitting parameter and plotted in Figure 2 as a function of the ion concentration.

At low ion concentration, the polymer solubility is about 0.5. The mixing term contributes to the network swelling, the particle size in this region (low $\Phi$) being controlled by the balance between the mixing and ionic terms (trying to swell the gel) and the elastic contribution (which contributes to particle deswelling).

At higher ion concentration, the polymer solubility decreases ($\chi$ raises to stabilize beyond ~0.5 M). Therefore, the presence of salt not only deswells the microgel through the ionic contribution to the total osmotic pressure but also affects the mixing term through changes of the polymer solubility. This adds an extra deswelling contribution coming from the coupling between the different contributions to $\pi_{total}$. This effect has been also observed for poly-NIPAM-(acrylic acid) microgel particles.[18]

Counterions moving into the particle by Donnan effect disturb the structured water surrounding the [poly(ViEtIm$^+$Br$^-$)] network. The reduction of polymer solubility in the presence of salt is explained in terms of the extent of the ions binding to water. The effective concentration of polymer increases (in the remaining "free" water) and tries to precipitate, thus releasing low entropy surface water. In summary, ions displace bound water, reduce the local order, the net entropy increases, and finally $\chi \approx |\Delta S|/k$ raises as shown in Figure 2.

**Wetting Kinetics.** Figure 3 shows several runs corresponding to different NaBr concentrations. Particle radius evolves to reach a final equilibrium size, $a_f$. The solid lines in Figure 3 are fits to the first five terms of the series expansion (eq 1). A salt-independent characteristic time is found to be $\tau = (0.29 \pm 0.02)$ s. This method to determine the characteristic time is very robust and practically independent of the approximation considered for the fitting procedure. This is due to the rapid convergence of the Fourier series describing the wetting process (eq 1). The inset in Figure 3 plots the reduced particle size $6/\pi^2[(a_f - a(t))/\Delta a_0] \approx \exp(-t/\tau)$. Data follow a decreasing exponential law showing that the first term in the Fourier series is the only relevant one describing the whole wetting process. Curves corresponding to different ion concentrations overlap on a unique salt-independent curve, with the slope corresponding to the common characteristic time $\tau$.

The wetting process, $a(t)$, is then controlled only by two equilibrium states: the collapsed and final swollen states ($\Delta a_0$ and $a_f$ in eq 1). The diffusion of the polymer network depends only on the ion concentration trough the final swollen state, $D \approx a_f^2$, and, consequently, it is exclusively controlled by the pressure the solvent exerts on the polymer mesh (osmotic terms in the equilibrium equation).

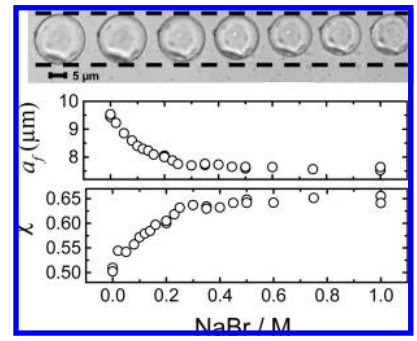


**Figure 2.** Final particle radius as a function of salt concentration and salt-dependent polymer solubility parameter. Pictures correspond to (from left to right): 0.0 (water), 0.02, 0.05, 0.1, 0.2, 0.5, and 1.0 M, respectively.

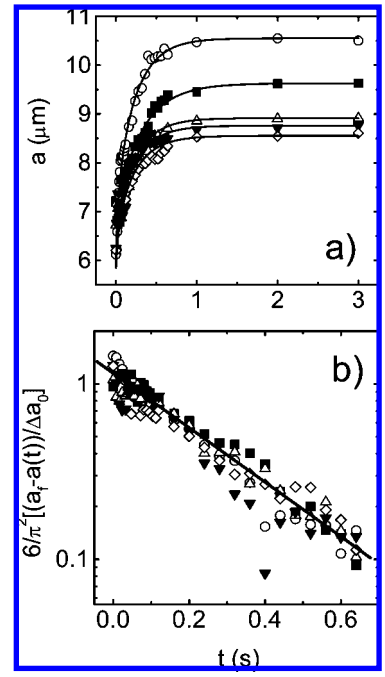


**Figure 3.** a) Particle size against time for different concentration of sodium bromide (from top to bottom): 0.0 M (○), 0.1 M (■), 0.2 M (△), 0.3 M (▼), and 0.5 M (◊). Fitting lines are solutions of equation 1 with 5 terms cut off. The characteristic process time is $\tau = (0.29 \pm 0.02)$ s. b) Scaling of the reduced particle size, showing the salt independent common characteristic time $\tau$.

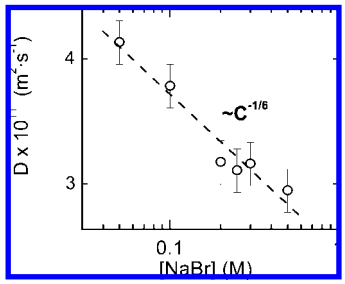


**Figure 4.** Network diffusion coefficient against NaBr concentration.

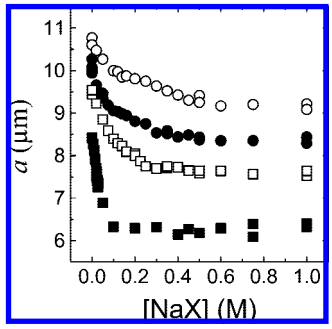


**Figure 5.** Plot of the size of PILs particle at several molar concentrations of the sodium halogenides solutions, [NaX]. X in NaX, refers to halogenides, $X^-$: (○) $F^-$ (●) $Cl^-$, (□) $Br^-$, and (■) $I^-$.

Figure 4 plots the network diffusion coefficient for different ion concentrations. A decreasing power law, $D \approx [NaBr]^{-0.16\pm0.02}$, is found. For pure water, the network diffusion coefficient $4.5 \times 10^{-11}$ m$^2$ s$^{-1}$ is similar of that reported for PNIPAM microgels ($\sim 4.2 \times 10^{-11}$ m$^2$ s$^{-1}$),[19,20] and far from that for self-diffusion of water molecules ($\sim 2.3 \times 10^{-9}$ m$^2$ s$^{-1}$ at 25 °C).[21]

The diffusion of a polymer network is determined by two factors: (i) the network elasticity through the bulk and shear modulus, $K$ and $\mu$, respectively, and (ii) the friction with the liquid crossing the network. Forces due to internal stresses (produced by volume changes and shear deformations) are balanced by the friction exerted by the liquid on the network. The diffusion of the polymer network is finally expressed as $D = (K + 4\mu/3)/f$, $f$ being the friction coefficient. Because the diffusion coefficient depends only on equilibrium states, changes of $D$ are related only to modifications of the network elastic properties. Any change of the local viscosity could change the network diffusion, but it is only possible through the characteristic time $\tau$ (thermodynamic equilibrium does not depend on viscosity), which is constant in the present case.

Decreasing diffusion coefficient in Figure 4 indicates that the polymer network reduces its elasticity as ion concentration increases, making the network softer. The microscopic mechanism responsible for this effect is not clear yet.

**Ion-Specific Wetting Behavior.** The influence of the ion nature is studied by inducing particle deswelling in the presence of electrolytes in the halogenide series: NaF, NaCl, NaBr, NaI. They share the cation $Na^+$, the counterions being located on the polymer network.

Figure 5 plots the particle size against increasing ionic concentration, $n$, for different electrolytes. Data correspond to pH = 5.88 at room temperature. At low $n$, the particle size decreases with increasing ion concentration, reaching a plateau. Deswelling is caused by the additional osmotic pressure the ions generate due to Donnan effect. The ionic term decreases with ion concentration. Such pressure competes against the elastic and mixing contributions, setting the final equilibrium size. At even higher salt concentration, the weak screening limit is exceeded, and direct electrostatic repulsions among charged polymer branches become dominant (as compared to the contribution of counterions located around the polymer). A final salt-independent particle size is thus reached.

The final particle size depends on anion nature as well as the $n$ value at which the plateau is reached. Both magnitudes quantify the solvency of the electrolyte. The deswelling capacity evolves as the ion size increases ($F^- < Cl^- < Br^- < I^-$) in opposite behavior to the well-know Hofmeister series, H.S.[22] The last orders, for instance, the effectiveness of ions to precipitate proteins. H.S has been recently checked for neutral thermosensitive microgels based on poly(*N*-isopropylacrylamide).[23] The authors found a clear correlation between the deswelling capacity of the ions and their chaotropic (structure breaking) or kosmotropic (structure making) nature. The halogenides follow strictly the H.S for neutral polymer network, just the opposite behavior observed in this Article.

The difference between both systems lies on the presence of charged groups arising from the amine functionalities. This adds an extra electrostatic interaction with respect to neutral polymer particles. To understand the observed behavior, we will consider the effect of the ions over three interactions present in imidazolium-based minigels: (i) polymer−polymer and polymer−counterion (counterion binding) electrostatic interactions, (ii) hydrophobic interaction among nonpolar groups, and (iii) polymer−polymer and polymer−water molecules hydrogen bounds.

In addition, ions influence the electrostatic interaction in two ways: (i) by screening of the Coulombic repulsions among charged groups, and (ii) through counterion binding. The first one is nonspecific for ions and depends on ionic strength and valence. Thus, this influence does not explain the experiments because they show a clear dependence on the ion nature. The effect of the ions on the polymer−anion electrostatic interaction (counterion binding) is however ion-specific. The specificity agrees with Desnoyer's model,[24] which establishes that solutes with similar hydration interact favorably, while unequal hydration drives to repulsive forces between them. In this model, the hydration enthalpy, $\Delta H_h$, quantifies the solute hydration degree. $\Delta H_h = -320$ kJ/mol for $NH_4^+$ (they are present when imidazole amine groups protonate). $\Delta H_h$ values for our anion series are well-known: $I^- = -300$, $Br^- = -345$, $Cl^- = -376$, $F^- = -519$ (kJ/mol). For weakly hydrated charged groups (as $NH_4^+$), counterions with low ionic hydration will be better deswelling agents that counterions bearing strong hydration. Consequently, hydration enthalpy let us to classify the deswelling capacity of anions in the series, $F^- < Cl^- < Br^- < I^-$.

Figure 6a plots the size of minigel particles against the counterion hydration enthalpy, $\Delta H_h$, for different ionic concentrations. The stronger interaction among anions and charged groups (or the favorable distribution of the electrolyte into the gel phase) provokes an important deswelling. The specific electrostatic interaction driven by ionic hydration increases deswelling for anions weakly hydrated. It also explains the fact that the salt-independent size is reached at smaller salt concentrations in the order established at the series.

Figure 6b plots the particle size versus salt concentration in the deswelling region, showing decreasing scaling laws. For polyelectrolyte gels,[25] swelling comes from the solely competition between elastic and ionic contributions. In this case, the exponent reaches the limit value −0.2. This limit was never observed in the present system due to the presence of an

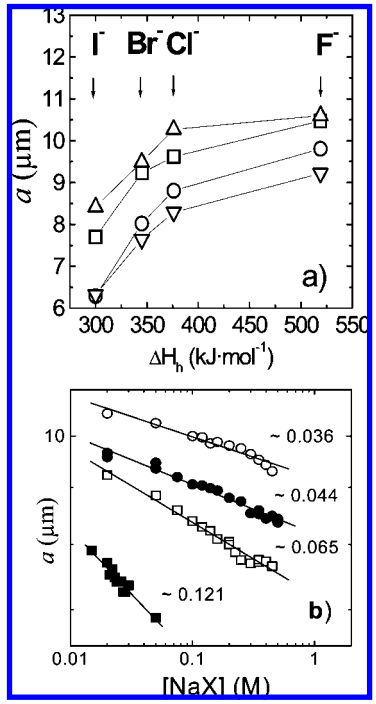


**Figure 6.** a) Plot of particle size versus hydration enthalpy at different salt concentrations, 0.0 M (△) 0.02 M (□), 0.20 M (○), 1.0 M (▽); b) Ion-specific de-swelling process of the PILS particles. The exponent α, $a \sim n^{-\alpha}$, accounts for the de-swelling capacity of the different anions, $F^-$ (○), $Cl^-$ (●), $Br^-$ (□), and $I^-$ (■).

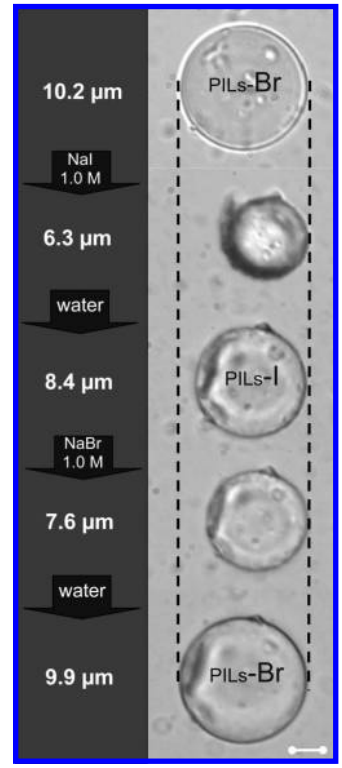


**Figure 7.** Pictures of the PILS particles showing the reversible ion exchange between $Br^-$ and $I^-$ ions. Electrolyte concentration is 1.00 M in all states. Reference bar corresponds to 5 μm.

additional mixing contribution to particle swelling (see Figure 2). Deswelling (Figure 6b) shows different decreasing exponents as the extent of the ion-specific electrostatic screening changes.

The mixing term accounts for the hydrophobic and hydrogen interactions. Force strength changes as a consequence of the interaction between ions and the water structured around the polar and nonpolar polymer groups. It depends on the kosmotropic or chaotropic character of the ions and would result in a series opposite to that obtained in this Article. It means that the dominant interaction must be electrostatic, both specific and nonspecific. The first contribution forms an ion-pair among charge groups and counterions and defines the series order.

**Anion Exchange.** The interaction between anions and PILs particles is shown to be reversible, which allows exchanging the halogenides between them in a reversible way. The exchange is described in simple terms with the chemical equation:

$$\text{Pils-X1} + \text{X2} \rightleftarrows \text{Pils-X2} + \text{X1}$$

where X1 and X2 are the halogenides 1 and 2. Figure 7 shows a sequence of pictures in which the ion exchange between $Br^-$ and $I^-$ ions becomes apparent. Particle size corresponds in every case to that displayed in Figure 5 at maximum salt concentration. The size for PILS-Br is recovered after addition of NaBr over PILS-I minigel. Ion exchange was observed for all halogenides. This property is of paramount importance for designing mini-devices such fuel cell, resins of exchange ions, and so on.

## Conclusions

In this Article, cross-linked imidazolium-based [poly($ViEtIm^+$ $Br^-$)] microparticles are synthesized, and their wetting properties are studied by optical microscopy, after addition of sodium halides. Particles show ion specificity and ion-exchange reversibility. The experimental particle equilibrium size is contrasted against the Flory−Huggins prediction with an extra ionic term accounting for the mesh charge and ion redistribution. This model describes fairly well the experiments showing salt-dependent polymer solubility for imidazolium-based minigels. The swelling kinetic is tracked using a high speed camera. A salt-independent characteristic wetting time is calculated by the Tanaka kinetic model to be $\tau = (0.29 \pm 0.02)$ s. The network diffusion coefficient follows decreasing power law with salt concentration. This behavior indicates that the polymer network reduces its elasticity as ion concentration increases, making the network softer. In addition, ion-specific wetting is found. Deswelling capacity evolves as the ion size increases ($F^- < Cl^- < Br^- < I^-$) in opposite behavior to the Hofmeister series. This finding is explained by the effect of the ions on the polymer−anion electrostatic interaction (counterion binding), which is ion-specific and is described by Desnoyer's model. The interaction between anions and PILs particles is shown to be reversible, which allows exchanging halogenides between them in a reversible way.

**Acknowledgment.** This work was supported by the Ministerio de Educación y Ciencia (Spain) under project MAT2006-13646-C03-02 and Junta de Andalucía under "Excellence Project": FQM-02353. I.J.S. is thankful for a fellowship from the INEST Group. J.R.-R. thanks the Ramón Areces Foundation for a postdoc fellowship.

## References and Notes

(1) Salamone, J. C.; Israel, S. C.; Taylor, P.; Snider, B. *Polymer* **1973**, *14*, 639.
(2) Ohno, H.; Ito, K. *Chem. Lett.* **1998**, 751.
(3) Yoshizawa, M.; Ohno, H. *Electrochim. Acta* **2001**, *46*, 1723.
(4) Kudo, T. In *The C.R.C. Handbook of Solid State Electrochemistry*; Gellings, P. J., Bouwmeester, H. J. M. Eds.; CRC Press, Inc.: Boca Raton, FL, 1997.

(5) Seki, S.; Ohno, Y.; Kobayashi, Y.; Miyashiro, H.; Usami, A.; Mita, Y.; Tokuda, H.; Watanabe, M.; Hayamizu, K.; Tsuzuki, S.; Hattori, M.; Terada, N. *J. Electrochem. Soc.* **2007**, *154*, A173.

(6) Wegner, G. *Polym. Adv. Technol.* **2006**, *17*, 705.

(7) Tanaka, T.; Fillmore, D. J. *J. Chem. Phys.* **1979**, *70*, 1214.

(8) Suarez, I. J.; Fernandez-Nieves, A.; Marquez, M. *J. Phys. Chem. B* **2006**, *110*, 25729.

(9) Kim, S.; Jung, Y.; Park, S. J. *Electrochim. Acta* **2007**, *52*, 2116.

(10) Marcilla, R.; Sanchez-Paniagua, M.; Lopez-Ruiz, B.; Lopez-Cabarcos, E.; Ochoteco, E.; Grande, H.; Mecerreyes, D. *J. Polym. Sci., Part A: Polym. Chem.* **2006**, *44*, 3958.

(11) Ruckenstein, E. *Polym. Synth./Polym. Catal.* **1997**, *127*, 1.

(12) Flory, P. J. *Principles of Polymer Chemistry*; Cornell University Press: London, 1953.

(13) Hirotsu, S. *Phase Trans.* **1994**, *47*, 183.

(14) Barrat, J. L.; Joanny, J. F.; Pincus, P. *J. Phys. II* **1992**, *2*, 1531.

(15) Hiemenz, P. C.; Rajagopalan, R. *Principles of Colloid and Surface Chemistry*, 3rd ed.; Marcel Dekker: New York, 1997.

(16) Shibayama, M.; Tanaka, T. In *Advances in Polymer Science*; Dusek, K. Ed.; Springer-Verlag: Berlin, 1993; Vol. 109, p 1.

(17) Shibayama, M.; Takata, S.; Norisuye, T. *Physica A* **1998**, *249*, 245.

(18) Capriles-González, D.; Sierra-Martín, B.; Fernández-Nieves, A.; Fernández-Barbero, A. *J. Phys. Chem. B*. Accepted.

(19) Hellweg, T.; Kratz, K.; Pouget, S.; Eimer, W. *Colloids Surf., A* **2002**, *202*, 223.

(20) Sierra-Martín, B.; Romero-Cano, M. S.; Cosgrove, T.; Vincent, B.; Fernández-Barbero, A. *Colloids Surf., A* **2005**, *270*−*271*, 296.

(21) Mills, R. *J. Phys. Chem.* **1973**, *77*, 685.

(22) Kunz, W.; Henle, J.; Ninham, B. W. *Curr. Opin. Colloid Interface Sci.* **2004**, *9*, 19.

(23) Lopez-Leon, T.; Fernandez-Nieves, A. *Phys. Rev. E* **2007**, *75*, 011801.

(24) Desnoyers, J. E.; Arel, M.; Perron, G.; Jolicoeur, C. *J. Phys. Chem.* **1969**, *73*, 3346.

(25) Fernandez-Nieves, A.; Fernandez-Barbero, A.; de las Nieves, F. J. *J. Chem. Phys.* **2001**, *115*, 7644.

JP802761Y